

GT2013-95727

FAULT TOLERANT SUPERVISION OF AN INDUSTRIAL GAS TURBINE

Emil Larsson*, Jan Åslund, Erik Frisk, Lars Eriksson
Div. of Vehicular Systems, Dep. of Electrical Engineering
Linköping University, Linköping, Sweden
Email: {lime, jaasl, frisk, larer}@isy.liu.se

ABSTRACT

Supervision of the performance of an industrial gas turbine is important since it gives valuable information of the process health and makes efficient determination of compressor wash intervals possible. Slowly varying sensor faults can easily be misinterpreted as performance degradations and result in an unnecessary compressor wash. Here, a diagnostic algorithm is carefully combined with non-linear state observers to achieve fault tolerant performance estimation. The proposed approach is evaluated in an experimental case study with six months of measurement data from a gas turbine site. The investigation shows that faults in all gas path instrumentation sensors are detectable and isolable. A key result of the case study is the ability to detect and isolate a slowly varying sensor fault in the discharge temperature sensor after the compressor. The fault is detected and isolated before the wash condition of the compressor is triggered, resulting in fault tolerant estimation of compressor health parameters.

1 INTRODUCTION

In industrial gas turbines, deterioration of components throughout the gas path is commonly occurring and contributes to overall performance degradation of the engine. Monitoring and supervision of performance degradation is a widely studied topic in the gas turbine diagnosis research field, see, e.g., [1, 2, 3]. With reliable performance estimations, the work for the service engineers to efficiently plan service and maintenance of the gas turbine can be significantly simplified. In papers [4, 5], several mechanisms which cause degradation in gas turbines are presented. The major contribution of degradation mechanisms in an industrial gas turbine is *fouling*. The fouling is caused by small particles and contaminants in the air that are caught by the compressor.

Performance degradation in the gas turbine is naturally occurring and so is faults in the sensors mounted on the gas turbine. It can be observed that it may be difficult to separate sensor faults from performance degradation and thereby get false alarms for sensor malfunction or premature cleaning of the compressor. This is caused by the fact that the error in the performance model increases with a high degree of deteriorated components which can trigger a sensor fault alarm [6]. In [7, 8], an investigation of performance degradation in industrial gas turbines using health parameters and experimental data is evaluated. These case studies show good estimation of compressor degradation using experimental data from a site during a time period of six month.

Problem Statement and Motivation

A fundamental problem with the method presented in [7, 8] appears when a sensor or an actuator fault is present simultaneously the performance degradation is estimated. For example, the efficiency of the compressor is especially sensitive to a slowly varying fault in the sensor which measures the discharge temperature of the compressor. A fault in this temperature sensor can result in an unnecessary early compressor wash or in a compressor wash which is performed too late. This phenomenon is shown in Fig. 1 where the estimated health parameters in the compressor are plotted during a time period of six months. A compressor wash is initiated when the estimated efficiency has dropped about 2–3% and the solid line in Fig. 1a shows a wash at day 144. However, with a 5% fault in the sensor, the estimate shown by the dotted line in Fig. 1a indicates that the compressor would be washed at day 83 which is two months early. Thus, it is clear that sensor faults could result in unreliable estimates of compressor wash intervals.

Another problem with the method in [7] is that sensor or actuator faults are only visible during the transient, i.e., while

*Address all correspondence to this author.

the fault develops. When the fault has reached a stationary value, its effects can not be observed in the measurements. A typical appearance of a residual that describe this phenomenon is shown in Fig. 1c where it is clear that the residual indicates a fault during the transient, but after $t = 120$, the residual goes back to zero again.

The main objectives of this work are: (i) extend the earlier developed supervision system for industrial gas turbines in [7, 9] to diagnose slow varying sensor or actuator faults while simultaneously estimating the performance degradation, and (ii) evaluate the diagnosis system on experimental data.

2 EXPERIMENT SETUP

At the current site, the gas turbine is a 1-shaft and 2-shafted gas turbine with a specific power of 29 MW. Since the gas turbine is 2-shafted, there is no mechanical connection between the gas generator and the power turbine. This gives the opportunity to adjust the speed of the power turbine independently of the gas generator speed. Thus, a typical usage for this type of gas turbine is a mechanical drive application. In these applications, the power turbine is connected to a driven component such as a pump or an external compressor.

In the evaluation of the FDI system, an experimental data set used for control and monitoring is available. The data is from a mechanical drive site and the signals are collected at different cross sections throughout the gas path. The cross sections are numbered from low to high numbers, where the low numbers represent the inlet of the gas turbine. Before the measurements are used in the FDI system some sub-sequences from the whole data set are removed. The removed sub-sequences relate to: (i) the start and stop of the gas turbine, and (ii) occasionally frozen sensors values. The sequences where the gas turbine is not running at operational conditions are removed since the diagnosis model, used in the FDI system, is not valid during these conditions. Sensors which are occasionally frozen are assumed to be non-fault (since the phenomenon is uncommon) and are therefore removed from the sequence. The original data set has a sample time of 5 min. To reduce the number of data points, the data is re-sampled with a sample time of 120 min. The total length of the data set is about six month. In the evaluation, the data set is divided into the two groups: (i) input signals, and (ii) output signals which are used in the FDI system.

Input Signals

The input signals to the diagnosis model are divided into two groups. The first group consists of: pressure p_0 , temperature T_0 , and relative humidity ϕ_0 of the ambient air. These signals are assumed to be non-faulty and are used to determine the gas properties of the ambient air. The second group of input signals are: mass flow of fuel m_f , and power generated by the application P_A . The signals in the second group may have a faulty value which should be diagnosed by the FDI system. These signals are called actuator signals in the sequel although they are measurements.

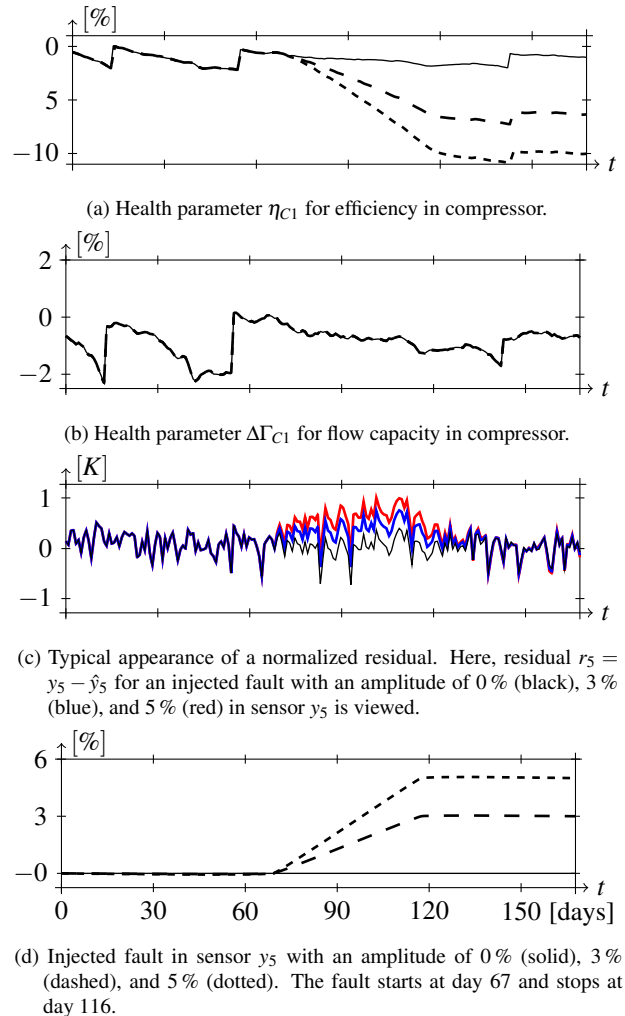


FIGURE 1: Health parameter estimation when a slow varying fault appears in sensor y_5 (discharge compressor temperature). The compressor is washed at day 15, 56, and 144. An appearance of a sensor fault suggest a compressor wash at day ~ 83 .

Output Signals

The output signals, used in the diagnosis model, are the measured quantities of: (i) temperature t_2 and pressure p_2 before compressor, (ii) temperature t_3 and pressure p_3 after compressor, (iii) temperature t_7 and pressure p_8 after power-turbine, and (iv) speed of gas generator n_{C1} and power-turbine n_{T0} . A challenge with this specific product model is the absence of an instrumentation sensor between the two turbines. The lack of these type of sensors makes the diagnosis and monitoring procedure more difficult to perform. Similar gas turbines, launched by other manufactures, have thermocouples between the gas generator and the power turbine. Having ideal thermocouples in that cross-section should reduce the uncertainty of the gas path parameters in the gas generator. In Fig. 2, a schematic view of the gas turbine and its signals is shown.

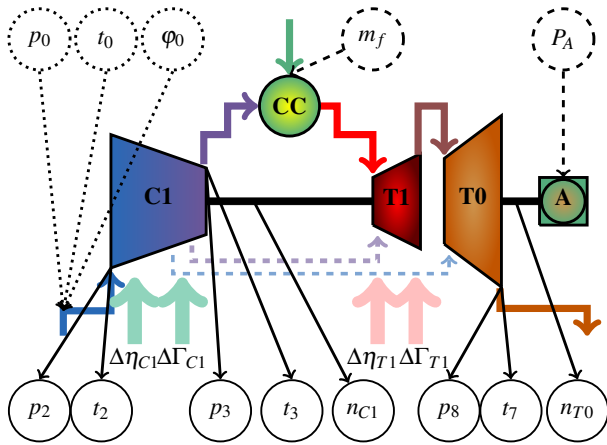


FIGURE 2: The gas turbine with the output signals (solid), the input signals (dashed), the input ambient signals (dotted), and health parameters (arrows). The secondary air flows, used to cool the first turbine blades, are shown with dashed arrows.

3 GAS TURBINE DIAGNOSIS MODELS

Each test quantity T_i in the FDI system is based on a physical model, i.e., the diagnosis model. The diagnosis model is derived from a gas turbine model used for performance calculation, i.e., the performance model. The performance model is validated against a reference model [10] developed by Siemens Industrial Turbomachinery AB in Finspång, Sweden. The two models used for diagnosis and performance calculation are first presented in [9] and are further elaborated in [8]. In the present work, the previous developed diagnosis model methodology is utilized where different configurations are considered. All these models are implemented in the object oriented and equation based language Modelica [11]. The simulations are performed using the tool Dymola marketed by Dassault Systems.

A key part of these gas turbine models is the involved media package GTLib. In GTLib, thermodynamic properties rely on the well-known NASA Glenn Coefficients [12] and are described using the states: pressure p , temperature t , and air/fuel ratio λ under the assumption that the combustion is lean, i.e., $\lambda \geq 1$. Throughout the gas path before the combustion, the air/fuel ratio is large (pure air) and after the combustion the air/fuel ratio is about 2–3 (exhaust gas). According to the cooling of the first blades in T1 and T0, gases with different air/fuel ratio are mixed together. Modelica provides libraries to construct very detailed gas models which can have an arbitrary number of species. All these species increase the number of equations and states in the global model which leads to increased computational complexity. In the reference model, the species in the gas mixture are specified using the mass fraction vector instead of the air/fuel ratio concept. This results in a number of states and equations which is strongly connected to the number of species in the gas mixture. Using the air/fuel ratio concept, the number of states and equations in the diagnosis and performance model can be reduced compared to the reference model.

The diagnosis model is a nonlinear dynamic model with algebraic constraints, i.e., a nonlinear differential algebraic equa-

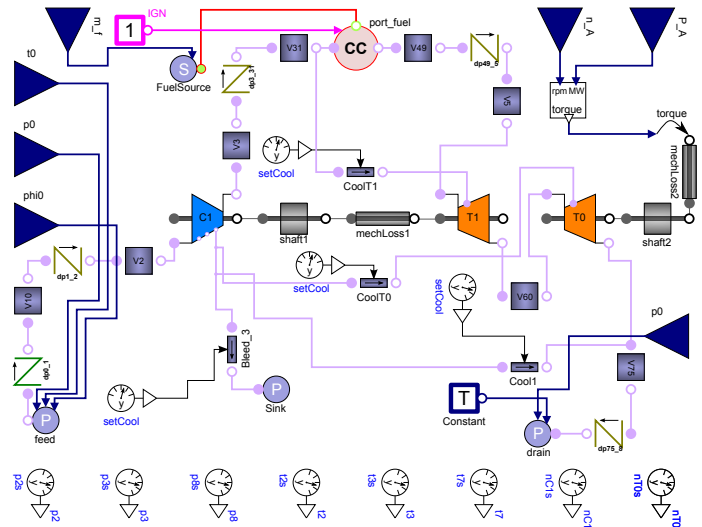


FIGURE 3: Graphical representation of the diagnosis model.

tion (DAE) model. In the characteristic calculations, corrected parameters according to [13] are utilized together with look-up tables. The diagnosis model is only valid during operational conditions, i.e., not valid during start and stop. The diagnosis model can be evaluated using a number of input signals, in contrast to the performance model which must be simulated together with the other components such as: a controller, a starter motor, a fuel system, and a driven component. The advantage with the diagnosis model is the ability to generate test quantities T_i used in the FDI system. The test generation procedure is first presented in [9] and then summarized in [8].

A graphical representation of the gas turbine diagnosis model is shown in Fig. 3. The intention with the figure is to give an overview of the component based diagnosis model together with the input and output signals. The number of equations in the model is about 1000 including about 30 dynamic state variables.

Health Parameters

A common approach in the gas turbine diagnosis research field to capture performance degradation is to introduce a number of physical based quantities named health parameters. The introduced parameters can be estimated with a number of techniques, see, e.g., [14, 6]. Two main disadvantages appear when using health parameters: (i) the observability of the system is affected, and (ii) a faulty sensor value may be captured by the health parameters. The maximum number of health parameters, which can be considered in the model due to the observability criteria, is restricted by the number of sensors. The maximum number of health parameters is equal to the number of sensors. In practise, this upper bound is much smaller and depends on where in the model the health parameters and sensors are located. In a case of a sensor fault, a faulty sensor value may be captured by the health parameter which was shown in Fig. 1. Especially slow

varying sensor faults can be difficult to detect in a noisy environment and disappear in the residuals when the fault has reached a stationary value. Thus, if no compensation for the sensor fault is done it is a balance between the ability to see a sensor fault in the residuals and the ability to get good estimation of the health, i.e., many health parameters in the model.

Since the compressor performance is important to supervise, two health parameters are introduced in the compressor to estimate degradation in: (i) isentropic efficiency $\Delta\eta_{C1}$, and (ii) mass flow of air $\Delta\Gamma_{C1}$. In case when no sensor or actuator faults have occurred, two more health parameters are used in the compressor turbine T1 to estimate degradation in: (iii) isentropic efficiency $\Delta\eta_{T1}$, and (iv) turbine flow number $\Delta\Gamma_{T1}$. The considered health parameters are injected in the performance characteristic equations:

$$\eta_i = f_{i,\eta}(\dots) + \Delta\eta_i, \quad \Gamma_i = f_{i,\Gamma}(\dots) + \Delta\Gamma_i \quad (1)$$

where η_i is the isentropic efficiency, Γ_i is the turbine flow number, and $f_{i,j}$ represents the nominal characteristic function with corrected quantities. Indices i represents the components: (i) CI in case of a sensor or actuator fault, and (ii) CI and TI if no sensor or actuator fault are present. Since the component deterioration is very slow relative to other gas turbine dynamics, the health parameters are modeled without dynamics and these constraints are added to the model:

$$\Delta\dot{\eta}_i = 0, \quad \Delta\dot{\Gamma}_i = 0 \quad (2)$$

for each inserted health parameter.

Sensor and Actuator Faults

Sensor and actuator faults f_i are modeled as unknown additive signals,

$$y_i = h_i(x) + f_{y_i} \quad (3a)$$

$$u_{new,j} = u_j + f_{u_j} \quad (3b)$$

$$\dot{f}_{y_i} = 0, \quad \dot{f}_{u_j} = 0 \quad (3c)$$

where $i = 1, \dots, 8$, $j = 1, 2, 3$, $h_i(x)$ are the measurement equations, and $u_{new,j}$ is the new input signal j . The diagnosed faults are assumed to be slow varying which gives a derivative equal zero. This has the attractive consequence that faults in actuators can be treated in exactly the same way as fault in sensors and performance degradation parameters.

Differential Algebraic Equation Form

The diagnosis model D_0 in the non faulty case has the DAE form:

$$F_{NF}(\dot{z}, z, u) = 0 \quad (4a)$$

$$y = h(z) \quad (4b)$$

$$z = (x^T, \Delta\eta_{C1}, \Delta\Gamma_{C1}, \Delta\eta_{T1}, \Delta\Gamma_{T1})^T \quad (4c)$$

and the diagnosis model D_k , in case of a fault, has the DAE form:

$$F_k(\dot{z}, z, u) = 0 \quad (5a)$$

$$y = h(z) \quad (5b)$$

$$z = (x^T, \Delta\eta_{C1}, \Delta\Gamma_{C1}, f_k)^T \quad (5c)$$

where indices $k \in [y_1, \dots, y_8, u_1, \dots, u_3]$. The vector x consists of the dynamic x_1 and algebraic x_2 variables. From these models, diagnosis test quantities are generated.

State Space Form

The purpose with the diagnosis model is to introduce faults and health parameters in an easy manner. Since the diagnosis model is equation based, where algebraic and dynamic constraints are mixed, some equation transformations are necessary to perform to get it into a state space form. The first step is to transform the set of equations in (4) – (5) automatically to a form which can be used in a diagnosis test quantity based on state space observers. To get the test equation, two main steps are performed: (i) check and reduce the DAE index of the system where Pantelides algorithm [15] is utilized, and (ii) find the overdetermined part and remove the exactly determined part using the Dulmage-Mendelsohn decomposition [16]. For these two steps, the structural model [17] of the diagnosis model is used. The test equations of diagnosis model D_k in state space form are:

$$\dot{x}_1 = f_k(x_1, u) \quad (6a)$$

$$y = h_k(x_1) \quad (6b)$$

where x_1 is the dynamic variables, u is the known input signals, and y is the known measurements. The functions f_k and h_k have appropriate dimension. The indices k is the same as used in (4) – (5). In the vector x_1 , the health parameters and fault are included. For a more detailed overview of each step, see [8] since these transformation steps are not trivial.

4 OBSERVER DESIGN

A common solution in the gas turbine diagnosis literature to estimate health deterioration is to use state space observers. The observers are often Kalman based which can be linear [14] and nonlinear [18, 19, 20]. The main objective in this section is to design an observer in the form:

$$\dot{\hat{x}} = f(\hat{x}, u) + K(y - \hat{y}) \quad (7a)$$

$$\hat{y} = h(\hat{x}) \quad (7b)$$

for each diagnosis model D_i in (4) – (5). The functions f and h can be non-linear, u represents the input signals, y represents the measurement signals, and K is the observer gain which can

be considered as a design parameter. A special type of a non-linear Kalman filter are a *Constant Gain Extended Kalman Filter* (CGEKF) [21]. In the paper, the robustness and stability of the observer are also investigated. For this kind of filters, the K matrix is constant and calculated for a given stationary point together with the noise matrices Q and R . For the diagnosis tests, K is calculated for the linearization of system (6). The R matrix is diagonal and is given the noise variance according to Tab. 1 for each diagonal element. The Q matrix is also diagonal where the elements representing the model uncertainty of each state variable. Especially the states variables of health parameters and faults have small uncertainty variance, i.e., the dynamics get slow for these estimation parameters.

TABLE 1: Standard deviation σ of measurement noise in percent.

Sensor	Quantity	σ
y_2	t_2	0.05 %
y_7	n_{C1}	0.1 %
y_1, y_2, y_3	p_2, p_3, p_8	0.2 %
y_5, y_6, y_8	t_3, t_7, n_{T0}	0.2 %

Before the observers are generated, it is necessary to check if the states are observable. Here, the structural observability criteria in [22] of the linearization of system (6) is considered. For each diagnosis model D_k in (4) – (5), a Kalman filter CGEKF $_i$ is generated. These Kalman filters are then gathered in a filter bank which is a part of the FDI system shown in Fig. 5.

5 FAULT ISOLATION METHOD DESCRIPTION

The main objective is to design a fault tolerant FDI system of an industrial gas turbine application using a bank of Kalman filters. The FDI system should diagnose single sensor or actuator faults. The Kalman filters are used to estimate the outputs \hat{y} and combine these outputs with the real measurement signals y to get residuals. These residuals are then filtered and compared with a given threshold value, which results in a logical test quantity T_i . The test quantities T_i are then used in the fault isolation logical component DIAG where the correct diagnoses are determined. These components create the FDI system where the inputs are the known quantities such as sensor and actuator signals. The output is a set of diagnoses which are consistent with the observations. The FDI system is based on hypothesis testing and there is one hypothesis for each sensor and actuator failure. Such an approach is standard in general diagnosis methodology [17] and similar approach was also utilized in [9].

In the actual application, let H_i denote the hypothesis that the sensor y_i or actuator u_{i-8} is faulty and let H^0 denote the null-hypothesis that no sensors or actuators are faulty. For each fault hypothesis H_i the test quantity T_i is designed, given the diagnosis

model D_i , where an additional state variable is introduced in the measurement sensor y_i or in the actuator signal u_j . If the hypothesis H_i is true, all filters except CGEKF $_i$ in T_i can not capture the faulty sensor or actuator value and the estimations have ideally a large error. If the hypothesis H_i is true, the estimator CGEKF $_i$ is used to supervise the performance, and if the hypothesis H^0 is true, the estimator CGEKF $_0$ is used.

Residuals

The output from each Kalman filter is an estimation of the state variables \hat{x} and the sensor values \hat{y} . The estimated sensor values from each filter are used to construct residuals in the form:

$$r_{i,j} = (\hat{y}_{i,j} - y_{i,j}) / \sigma_{i,j} \quad (8)$$

where $i \in [0, \dots, 10]$, $j \in [1, \dots, 8]$, $r_{i,j}$ are the residual, and $\sigma_{i,j}$ is the standard deviation of $r_{i,j}$ in the fault free case. Since the measurement sequence is available offline, the residuals can be normalized with the standard deviation of the residuals in the fault free case. With this normalization, the signals are in the same interval.

CUSUM Algorithm

For change detection in signals, low-pass filtering combined with a static threshold can be considered. A disadvantage with low-pass filtering is the time response for the detection of a fault. A more suitable choice for change detection is to use the CUSUM algorithm [23]. The CUSUM algorithm, together with a static threshold $J_{i,j}$ are used to decide if the actual residual $r_{i,j}$ indicates an abnormal behaviour according to a sensor or actuator fault. The CUSUM test quantity $T_{i,j}$, for each residual, is computed:

$$T_{i,j}(t) = \max(0, T_{i,j}(t-1) + |r_{i,j}(t)| - v_{i,j}), \quad T_{i,j}(0) = 0 \quad (9)$$

where t is time, $i \in [0, \dots, 10]$, $j \in [1, \dots, 8]$, $v_{i,j}$ is a tuning parameter to ensure that $T_{i,j}(t) < 0$ in the fault free case, and $|r_{i,j}(t)|$ is the absolute value of residual in (8). The threshold $J_{i,j} = J$ is equal for all CUSUM tests since the the normalization in (8) was performed. The test quantity trigger an alarm if $T_{i,j}(t)$ exceeds the specified threshold J . The design parameter $v_{i,j}$ is tuned so the test does not give any unnecessary alarms in the fault free case. A good rule of thumb is that $v_{i,j}$ has the same order of magnitude as the residual $r_{i,j}$ in the fault free case, i.e., about 1.

Test Quantity $T_i(t)$

For each Kalman filter a test quantity $T_i(t)$ is generated (see Fig. 4). The test quantity of Kalman filter i is constructed as a logical or operation of the logical expression $T_{i,j}(t) > J$ for each CUSUM test in the filter i . This means that if any of the CUSUM tests $T_{i,j}(t)$ alarm, the logical test quantity $T_i(t)$ will also trigger an alarm.

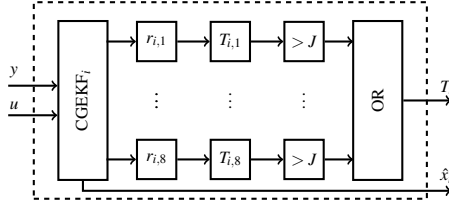


FIGURE 4: The logical test quantity T_i .

Diagnosis Procedure

In an ideal case, if a slow varying fault is present in sensor signal y_j all test quantities except $T_i(t)$ should trigger an alarm. In practise, this is not always true since, e.g., measurement noise, fault size, and model uncertainty are always present together with the tuning procedure of the CUSUM tests $T_{i,j}(t)$. All these things affect the alarm ability and reaction rate of each test quantity.

Another aspect is the ability of the method to discriminate between different faults, i.e., isolability properties. It will be shown that faults in the speed sensor y_8 of the power turbine is difficult to isolate from a fault in the power sensor u_2 of the application.

No Fault Hypothesis Most of the time, when the system has no sensor or actuator faults, no tests triggers. To reduce unnecessary false alarms, the condition when the system is faulty is tightened. A design parameter is chosen for how many tests that need to trigger before an alarm is generated. Thus, if no more than 5 tests alarm it is assumed that the NF diagnosis is most probable. When the no fault hypothesis H^0 is true, the CGEKF₀ is used to supervise the performance, i.e., the Kalman filter which utilizes 4 health parameters and no sensor or actuator faults. The CGEKF₀ filter is utilized in the fault free case for best performance since extra estimation parameters in the sensors always affect the health estimation negative. Also the performance degradation of the compressor turbine may be relevant to supervise.

Unique Diagnosis Statement If all tests except test $T_i(t)$ alarm, a unique diagnosis can be selected. When a unique diagnosis is decided, the performance is supervised with the observer CGEKF_{*i*}. This Kalman filter utilizes 2 health parameters to supervise the degradation in the compressor. In this case, the amplitude of the sensor or the actuator fault can be estimated with the filter.

Multiple Diagnosis Statement A unique diagnosis is obtained if all tests except one trigger an alarm. For each test that exceeds its threshold, a diagnosis candidate from the diagnosis set is excluded until only one candidate remain. However, in certain operating conditions or when the faults are particularly small, it may be the case that not all tests alarm which they ideally should do. In such a situation, it can be concluded that there

is a fault but the algorithm can not uniquely isolate the faulty component. In such a situation, for example when all except 3 tests give an alarm, it can be useful to alert the gas turbine operator and generate a so called *soft alarm*, indicating that it is not possible to isolate the actual fault, but 3 diagnosis candidates are available. The value 3 is chosen here since its gives a good balance between false alarms and missed fault detections for the considered data set.

When a soft alarm is generated the operator can make three main decisions for continued operation: (i) wait until a unique diagnosis is identified, (ii) check the fault candidates. Some candidates cannot be isolated, e.g., f_{y_8} and f_{u_2} . In this case, it doesn't matter which of the observers (not alarming) that are used for health parameter estimation since it is a strong connection between the faults, and (iii) further investigation of the health parameters in the observers which are not alarming. Perhaps give all filters except one strange estimations of the health parameters. A remaining choice is to stop the operation and replace all possible faulty sensors.

No Diagnosis Statement Finally, if all tests alarm no diagnosis is possible under a slow varying single fault assumption. If this case appears in connection with a diagnosis, it can be assumed that the previous diagnosis is valid. If this case occurs during a longer period of time, it can be a multiple fault which is not diagnosable with the presented method. The design parameters $v_{i,j}$ and threshold J can also be tweaked so the test is to sensitive. If an abrupt fault is introduced, all test quantities will be triggered during a period of time. This happens since the extra parameter needs time to capture the fault value. In an ideal case, the correct diagnosis is obtained after this period of time.

Method Summary

The fault isolation method can be summarized in:

1. Calculate the residuals $r_{i,j}(t)$ according to (8), where $i = 1, \dots, n, j = 1, \dots, m, n$ is the number of Kalman filters, and m is the number of measurement signals.
2. Compute the CUSUM test $T_{i,j}(t)$ of each residual and compare it with a static threshold J according to (9).
3. Obtain the test quantity $T_i(t)$ using a logical or operation of all $T_{i,j}$ where $j = 1, \dots, m$.
4. If no more than six tests triggers an alarm, use the CGEKF₀ filter with 4 health parameters to estimate the performance.
5. If all tests except one are triggered, a unique diagnosis is obtained. The test which is not triggered can be used to supervise the performance and estimate the sensor fault. If the diagnosis is not unique, check which tests are not alarmed and an idea is to investigate how the health parameters are affected. Another alternative is to wait to see if a unique diagnosis can be obtained.

The FDI system is shown in Fig. 5 where also the interaction with the other gas turbine components are shown.

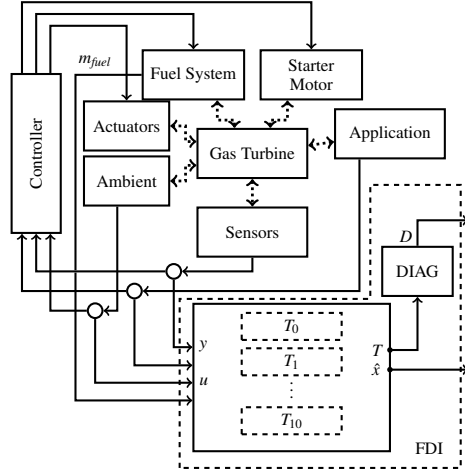


FIGURE 5: The gas turbine experiment platform, where a bank of test quantities T_i are used together with a fault isolation logic component (DIAG). These components formed the Fault Detection and Isolation (FDI) system. Ordinary signals are represented with solid arrows, and physical based connections are represented with dotted arrows.

6 EXPERIMENTAL CASE STUDY

In this section, the FDI system is evaluated on experimental data from a gas turbine site. The environment air at this site consists of a high grade of air pollutions such as: sand, salt, oil, and other contaminations which affect the compressor performance. This results in compressor fouling frequently, so the customer needs to shut down the gas turbine for maintenance quite often. In Fig. 1 (solid line), the compressor efficiency and mass flow through the compressor is estimated with an observer plotted for a time period of six month. This observer was developed in [7,8] with two typical disadvantages when a sensor fault occur: (i) the health parameters are affected by a sensor or actuator fault (Fig. 1a), and (ii) the possibility to detect the fault in the residuals disappears when the fault go back to a constant value (Fig. 1c). In [9], a fault isolation method was presented. A problem with the purposed technique is the inability to detect slow varying sensor fault since the health parameter capture the faulty sensor value. This results in test quantities which are not alarming. Another disadvantage with the method is the ability to decouple actuator fault in an easy manner. In the present work, actuator faults are modeled in the same way as a sensor fault which is preferred.

In the measurement sequence, compressor washes are performed at day: 15, 56, and 144. Before a compressor wash the efficiency has degraded 2–3 % from the nominal value. As shown in the figure, the compressor efficiency is especially sensitive to a fault in the discharge temperature sensor y_5 . Therefore, it is important to detect and isolate the sensor fault before the efficiency has degraded 2–3 %, i.e., at day 83. The focus in the case study is on detection and isolation of faults in the sensors: y_2 (compressor discharge pressure p_3), y_5 (compressor discharge temperature t_3), and y_6 (exhaust gas temperature t_7). These sensor faults are

shown here because they are important for the process and early investigations show that they are difficult to detect and isolate.

For the evaluation of FDI system, a ramp fault is injected in each measurement sequence. The injected fault corresponds to the appearance seen in Fig. 1d. Each injected sensor fault is

TABLE 2: Fault modes and amplitude of injected sensor or actuator ramp faults in percent of the nominal values at the standard operational condition.

Fault Mode	Signal	Quantity	Amplitude	Duration
F_{NF}	-	-	-	-
$F_{t_2}, F_{t_3}, F_{t_7}$	y_4, y_5, y_6	t_2, t_3, t_7	3 (5) %	50 days
$F_{p_1}, F_{p_3}, F_{p_8}$	y_1, y_2, y_3	p_2, p_3, p_8	4 (5) %	50 days
$F_{n_{C1}}, F_{n_{T0}}$	y_7, y_8	n_{C1}, n_{T0}	5 %	50 days
F_{m_f}, F_{P_A}	u_1, u_2	m_f, P_A	5 %	50 days

denoted with a faulty mode F_i shown in Tab. 2 together with the fault amplitude in percent of the nominal value. The time scale of each fault is 50 days.

Sensor Fault in T3 with an Amplitude of 3 %

The proposed approach is first demonstrated on a particularly difficult fault case with a fault in sensor y_5 . The considered fault is a ramp with an amplitude of 3 % of the nominal value and is shown in Fig. 1d. The aim is to detect, and isolate the fault before the estimated performance has degrade more than the *compressor wash condition* which is about 2–3 %. Therefore have the injected faults an amplitude of > 3 %.

In Fig. 6, the residuals of CGEKF₂ filter in fault mode F_{t_3} are compared with the fault mode F_{NF} . The CGEKF₂ is selected in the example because the filter estimates a fault in the pressure sensor y_2 which measure the pressure in the same cross section. Thus, it is possible to expect that this parameter will pick up the injected sensor fault and make the detection problem difficult. In an ideal case when the model is different, all these residuals should differ from the nominal residuals. As shown in the figure, three of the residuals: $r_{2,1}$, $r_{2,3}$, and $r_{2,4}$ show only marginal changes. However, since it is sufficient that only one residual generates an alarm, the fault will be detected by the test. In Fig. 7 it clearly shows that the CUSUM test quantities based on $r_{2,5}$ and $r_{2,6}$ clearly give an alarm as expected.

The results for all tests T_i are presented in Fig. 8a-j. The Fig. 8k indicates when a soft alarm (red) and a unique diagnosis (blue) are obtained. The unique diagnosis is obtained when all tests except T_5 , corresponding to the correct fault mode, have generated an alarm. Thus, here the diagnosis system draws the correct conclusion. A soft alarm appears at day 90 if 2.5 % degradation is assumed for the compressor was conditions, which is about 5 days to late. The actual diagnosis at day 90 are: D_{t_3} , D_{t_7} , and D_{m_f} which means that tests: T_5 , T_6 , and T_9 have not

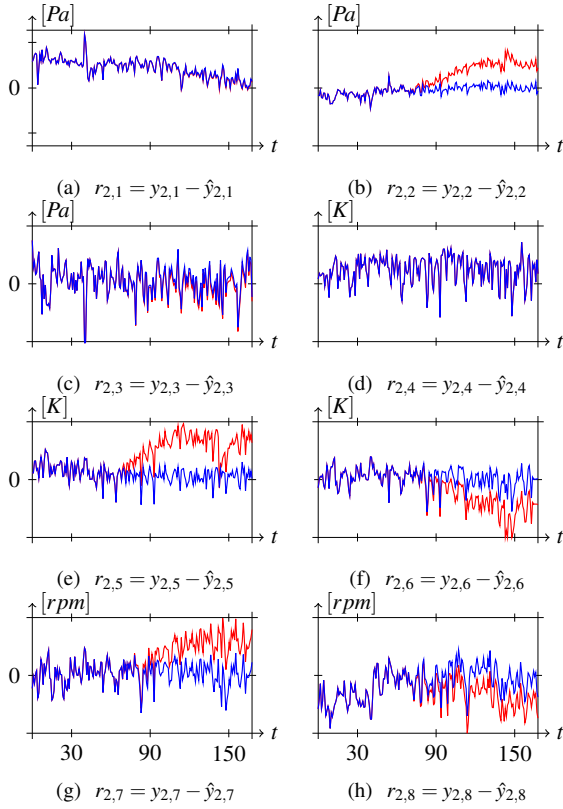


FIGURE 6: Residuals $r_{2,i}$ of the CGEKF₂ when a ramp fault of amplitude 3% (red) is injected into the measurement of y_5 are viewed together with residual where no fault (blue) is injected.

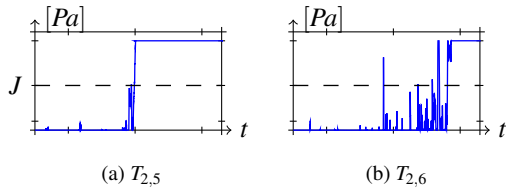


FIGURE 7: CUSUM tests of residuals $r_{2,5}$ and $r_{2,6}$.

triggered. At day 105, the unique diagnosis D_{T_3} is obtained. It is shown that some false alarms appear at day 45. The false alarm depends on an abrupt changes in two of the residuals, shown in Fig. 6a and 6c, for all CGEKF_s.

Fault Isolability

To investigate how the fault isolation procedure works for each fault mode, the evaluation presented in the previous section is generalized. A ramp fault with an amplitude according to Tab. 2 is injected in each measurement signal and an analysis corresponding to Fig. 8 is performed. The diagnosability for each fault mode is presented in Fig. 9. According to Fig. 9, the fault modes: F_{p_1} , F_{p_3} , F_{p_8} , F_{T_2} , F_{T_3} , $F_{n_{C1}}$, and F_{m_f} are isolable for the considered fault signals. Thus, all faults can not be isolated from each other. According to Fig. 9, a fault in the temperature sensor y_6 is not isolable from a fault in the mass flow sensor u_1 . However, it turns out that the opposite is true, a fault in u_1 is isolable from a

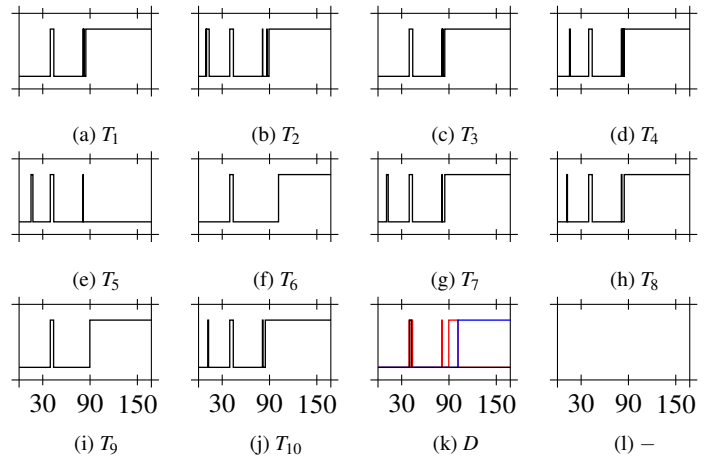


FIGURE 8: All test quantities T_i in the FDI system are shown when a fault in the sensor y_5 is injected. These tests result in a diagnosis candidate set D . When all tests except one exceeds its threshold a unique diagnosis statement (blue) is available. When all tests except 3 exceeds its threshold, a soft alarm (red) is generated. When all tests alarm (black) fault isolation is not possible. For the unique diagnosis, all tests except test T_5 alarm.

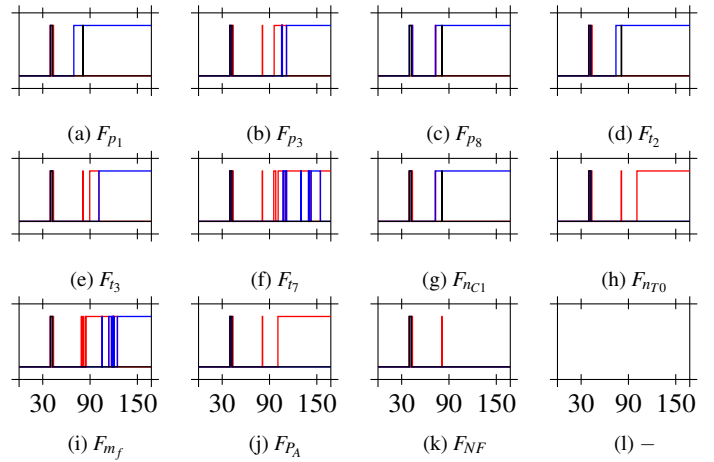


FIGURE 9: The figure shows all modes when the faults from Tab. 2 are added to the input/output signals. For the soft alarm (red) all test except 3 need to be triggered, and if all test except 1 triggered (blue) a unique diagnosis is obtained. If all tests trigger (black), the single fault diagnosis assumption is not valid.

fault in y_6 . None of the fault modes: $F_{n_{T0}}$, and F_{P_A} can be isolated from each other. For example, an extra estimation parameter in the power signal can capture a fault in the speed sensor, and vice versa.

Sensor Fault in p3, T3, and T7 with an Amplitude of 5%

The problem illustrated in previous section where it is not possible to uniquely isolate the faults is related to fault sizes; the bigger the amplitude of the faults are, the easier are they to de-

fect and isolate. To further illustrate this, faults in the sensors: y_2, y_5 , and y_6 with increased fault sizes (5%) are investigated. The diagnosis schemes for the faulty modes are shown in Fig. 10. The isolation property of F_{I3} increases, while a soft alarm is now

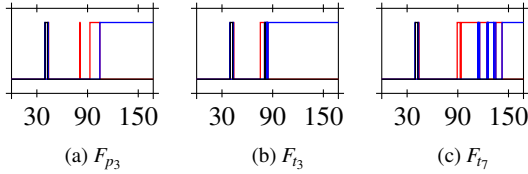


FIGURE 10: The diagnosis statements when the sensor faults in y_2, y_5 , and y_6 are increased to 5%.

generated at day 77 which is before the compressor wash condition is triggered. The faulty mode F_{I7} is now isolable, while the performance of F_{p3} is nearly the same as before. A fault in pressure sensor y_2 affect the health parameter estimation according to Fig. 11. Thus, since the health parameter increases it is enough to isolate the fault before the compressor wash is performed at day 144. The fault in y_2 is isolated at day 115.

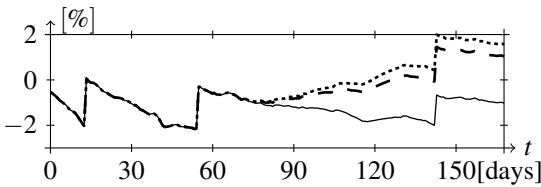


FIGURE 11: Health parameter estimation of $\Delta\eta_{C1}$ with the CGEKF₀ when a sensor fault in y_2 is present with amplitude: 0% (solid), 3% (dashed), and 5% (dotted).

Fault Tolerant Performance Estimation

The estimated states by the Kalman filters are used for: (i) supervision of performance degradation, and (ii) as input signals to the controller. The estimated states depend on the actual sensor or actuator fault mode of the system. When the null-hypothesis H^0 is valid, the states are estimated with the CGEKF₀ filter. In case when a unique diagnosis is achieved, the test which has not exceeds its threshold is used to estimate the states. The actual fault can also be estimated. In other cases, when a soft alarm is generated, any of the remaining tests can be used to estimate the states, i.e., the tests which have not exceed its threshold.

In Fig. 12, the health parameters are shown for the fault modes: F_{NF}, F_{p3}, F_{I3} , and F_{I7} . The estimated health parameters for the faulty modes are not so good as in the non faulty case, but it is clear that the estimates clearly outperform the initial situation shown in Fig. 1a and Fig. 11. A fault in y_5 has a strong influence on the health parameter $\Delta\eta_{C1}$ while a fault in y_6 is unaffected.

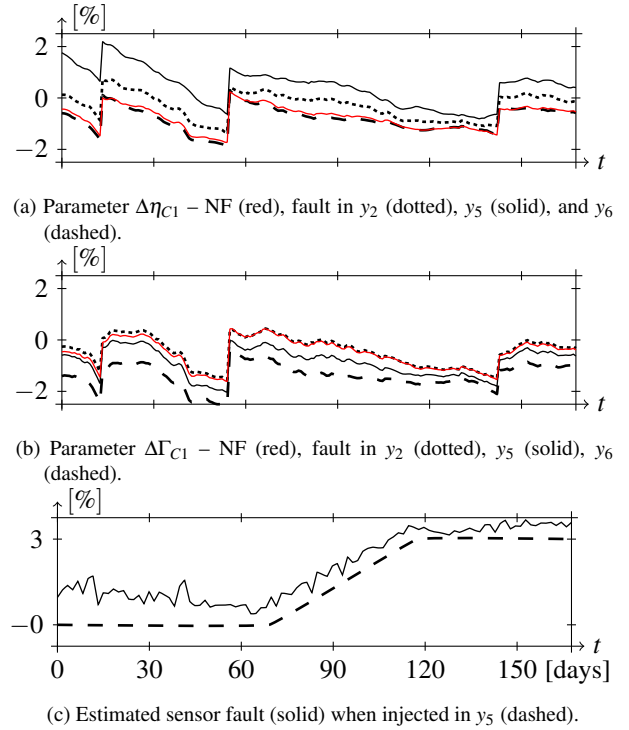


FIGURE 12: Health parameter estimations in the case of a fault.

7 CONCLUSION

An undetected sensor or actuator fault affects the performance estimation in an industrial gas turbine. Especially slowly varying sensor faults are difficult to detect and isolate. Thus, it is of great importance to have a FDI system which can estimate the performance even if a sensor or an actuator fault has occurred. The performance estimations are used to, e.g., decide if it is time to wash the compressor. It is desirable, if the sensor fault can be diagnosed before an unnecessary compressor wash is performed.

The developed FDI system consists of a bank of logical test quantities and a fault isolation component. A test quantity is designed for each fault mode and consists of a CGEKF which is used to detect abnormal behaviour in the residuals and estimate the performance using a number of health parameters. The advantage with the proposed method is the ability to consider actuator fault in the same manner as sensor faults. In a case of a fault, an extra parameter is used to estimate the fault at the same time as it compensates for the error in the residuals. This results in a test quantity which is not sensitive to the fault and is used to estimate the performance.

In the experimental case study, changes in all gas path parameters are detectable and isolable given the considered fault size. In the occurrence of a sensor fault and if a unique diagnosis statement is possible, the proposed algorithm switches to a specific Kalman filter that provides performance estimates that are not affected by the sensor fault. It is shown, using experimental data from a gas turbine site, that unnecessary stops according to faulty sensors can be avoided if the proposed approach is utilized.

ACKNOWLEDGMENT

The research has been funded by the Swedish Energy Agency, Siemens Industrial Turbomachinery AB, Volvo Aero Corporation, and the Royal Institute of Technology through the Swedish research program TURBOPOWER, the support of which is gratefully acknowledged.

NOMENCLATURE

FDI	Fault Detection and Isolation System
CGEKF	Constant Gain Extended Kalman Filter
C1	Compressor
T1, T0	Compressor- and power turbine
D_k	Diagnosis model k
λ	Air/fuel ratio
$\Delta\eta_i$	Health parameter of efficiency in comp. i
$\Delta\Gamma_i$	Health parameter of flow capacity in comp. i
p_2, p_3, p_8	Pressure at cross section i in [Pa]
t_2, t_3, t_7	Temperature at cross section i in [K]
n_{C1}, n_{T0}	Speed of C1 and T0 in [rpm]
y_1, y_2, y_3	Measurement signals of p_2, p_3, p_8
y_4, y_5, y_6	Measurement signals of t_2, t_3, t_7
y_7, y_8	Measurement signals of n_{C1}, n_{T0}
$r_{i,j}$	Residual of CGEKF i and sensor j
T_i	Test quantity i

REFERENCES

- [1] Aker, G. F., and Saravanamuttoo, H. I. H., 1989. "Predicting gas turbine performance degradation due to compressor fouling using computer simulation techniques". *Journal of Engineering for Gas Turbines and Power*, **111**(2), pp. 343–350.
- [2] Volponi, A. J., DePold, H., Ganguli, R., and Daguang, C., 2003. "The use of kalman filter and neural network methodologies in gas turbine performance diagnostics: A comparative study". *Journal of Engineering for Gas Turbines and Power*, **125**(4), pp. 917–924.
- [3] Doel, D. L., 2003. "Interpretation of weighted-least-squares gas path analysis results". *Journal of Engineering for Gas Turbines and Power*, **125**(3), pp. 624–633.
- [4] Diakunchak, I. S., 1992. "Performance deterioration in industrial gas turbines". *Journal of Engineering for Gas Turbines and Power*, **114**(2), pp. 161–168.
- [5] Kurz, R., Brun, K., and Wollie, M., 2009. "Degradation effects on industrial gas turbines". *Journal of Engineering for Gas Turbines and Power*, **131**(6), p. 062401.
- [6] Kobayashi, T., and Simon, D. L., 2003. *Application of a Bank of Kalman Filters for Aircraft Engine Fault Diagnostics*. NASA/TM-2003-212526.
- [7] Larsson, E., Åslund, J., Frisk, E., and Eriksson, L., 2011. "Health Monitoring in an Industrial Gas Turbine Application by Using Model Based Diagnosis Techniques". *ASME Conference Proceedings*, **2011**(54631), pp. 487–495.
- [8] Larsson, E., 2012. Diagnosis and Supervision of Industrial Gas Turbines. Tech. rep. LiU-TEK-LIC-2012:13, Thesis No. 1528, <http://urn.kb.se/resolve?urn=urn:nbn:se:liu:diva-75985>.
- [9] Larsson, E., Åslund, J., Frisk, E., and Eriksson, L., 2010. "Fault isolation for an industrial gas turbine with a model-based diagnosis approach". *ASME Conference Proceedings*, **2010**(43987), pp. 89–98.
- [10] Idebrant, A., and Näs, L., 2003. "Gas Turbine Applications using Thermofluid". In Proceedings of the 3rd International Modelica Conference, P. Fritzson, ed., The Modelica Association, pp. 359–366.
- [11] Modelica Association, 2007. The Modelica Language Specification version 3.0.
- [12] McBride, B. J., Zehe, M. J., and Gordon, S., 2002. Nasa glenn coefficients for calculating thermodynamic properties of individual species. Tech. Rep. TP-2002-211556, National Aeronautics and Space Administration (NASA).
- [13] Volponi, A. J., 1999. "Gas turbine parameter corrections". *Journal of Engineering for Gas Turbines and Power*, **121**(4), pp. 613–621.
- [14] Luppold, R. H., Roman, J. R., Gallops, G. W., and Kerr, L. J., 1989. "Estimating in-flight engine performance variations using kalman filter concepts". In 25th Joint Propulsion Conference, 2584-AIAA.
- [15] Pantelides, C. C., 1988. "The consistent initialization of differential-algebraic systems". *SIAM J. Sci. Stat. Comput.*, **9**(2), pp. 213–231.
- [16] Dulmage, A. L., and Mendelsohn, N. S., 1958. "Coverings of bipartite graphs". *Canadian Journal of Mathematics*, **10**, pp. 517–534.
- [17] Blanke, M., Kinnaert, M., Lunze, J., and Staroswiecki, M., 2003. *Diagnosis and Fault-Tolerant Control*. Springer.
- [18] Borguet, S., and Léonard, O., 2008. "A sensor-fault-tolerant diagnosis tool based on a quadratic programming approach". *Journal of Engineering for Gas Turbines and Power*, **130**(2), p. 021605.
- [19] Dewallef, P., Romesis, C., Léonard, O., and Mathioudakis, K., 2006. "Combining classification techniques with kalman filters for aircraft engine diagnostics". *Journal of Engineering for Gas Turbines and Power*, **128**(2), pp. 281–287.
- [20] Rausch, R. T., Goebel, K. F., Eklund, N. H., and Brunell, B. J., 2007. "Integrated in-flight fault detection and accommodation: A model-based study". *Journal of Engineering for Gas Turbines and Power*, **129**(4), pp. 962–969.
- [21] Safonov, M., and Athans, M., 1978. "Robustness and computational aspects of nonlinear stochastic estimators and regulators". *Automatic Control, IEEE Transactions on*, **23**(4), aug, pp. 717 – 725.
- [22] Shields, R., and Pearson, J., 1976. "Structural controllability of multiinput linear systems". *Automatic Control, IEEE Transactions on*, **21**(2), apr, pp. 203 – 212.
- [23] Page, E., 1954. "Continuous inspection schemes". *Biometrika*, **41**, pp. 100–115.